An appraisal of the mechanical, microstructural, and thermal characteristics of concrete containing waste PET as coarse aggregate

Gideon Bamigboye[a],[*], Karnik Tarverdi[b], Damola Adigun[a], Bassey Daniel[a], Uchechukwu Okorie[c], Joel Adediran[a]

[a] Department of Civil Engineering, Covenant University, Ota, Ogun State, Nigeria
[b] Department of Chemical Engineering, Brunel University, London, UK
[c] Department of Economics, Covenant University, Ota, Ogun State, Nigeria

ABSTRACT

This study assessed the workability, mechanical, microstructural, and thermal behaviours of concrete composed from recycled waste polyethylene terephthalate (PET) as a partial or full replacement for natural coarse aggregates. Workability and Compressive/Split tensile strength tests alongside microstructural and thermogravimetric analysis were performed. Results disclosed that the concrete's workability increased with increasing percentages of PET. The compressive strength increases with extended curing but decreases as the percentages of waste PET increased at different curing lengths. The PET-modified blends could not yield the target design strength for grade 25 concrete after 28 days. However, the 20% PET-modified mix reached the target strength for concrete grade 20. For all blends, increase in split tensile strength with curing lengths was observed, only the 20% PET-modified blend achieved suitable split tensile strength values. Microstructural analysis revealed that the 100% PET sample has a relatively irregular surface pattern with pores of about 2–4 μm, high quantities of Ca, and minor traces of O, C, Al, Si, Mg, and Na. While PC-20 had a much denser interface between the PET aggregates and the cement matrix with high percentage of Si, O, and Ca, and moderate to minor percentage of Al, Au, Na, and Mg. Thermal analysis showed that the 100% PET sample endured three transition stages. The research outcomes prove that heat-processed PET-modified concrete is suitable for structural applications due to its acceptable fresh, mechanical, microstructural, and thermal properties. Moreover, this alternative is eco-friendly and sustainable as it substitutes natural aggregates with waste plastics.

1. Introduction

The continuous manufacture and consumption of single-use plastics across the globe, in the past few decades, poses serious threats to the environment. The inadequate management and disposal of these plastic materials have resulted in soil and water contamination, and huge reductions in landfill capacity (Bamigboye et al., 2019). Plastics accounts for about 13% of the total municipal solid wastes (MSW) generated worldwide annually, it also accounts for 19.2% and 16.4% of total MSW landfilled and combusted, respectively. However, plastic recycling only accounts for 4.4% (US Environmental Protection Agency (USEPA), 2017). The global consumption of plastic which was about 5 million tonnes as of 1950, multiplied to about 100 million tonnes in 2001 (Islam et al., 2016), and about 359 million tonnes in 2018 (Statista, 2020). The rising trend for the generation of waste plastics is shown in

Fig. 1. Estimates by the US Environmental Protection Agency (EPA), 2017 projects that by 2050, the oceans could contain more indiscremenately disposed waste plastics than marine lifeforms.

Plastics can be classified into thermosetting plastic and thermoplastic-based on polymers thermoplastics can be melted and hardened through heating and cooling, respectively. They include polystyrene, polyethylene, polyethylene terephthalate (PET), polypropylene, and high-density polyethylene. Whereas, thermosetting plastics such as phenol-formaldehyde, polyurethane, epoxy resins, silicone, and vinyl ester cannot be re-hardened or re-melted through varying temperatures after initial formation (Panyakapo and Panyakapo, 2008; Siddique et al., 2008). PET polymer is a tough semi-crystalline with high mechanical strength, it offers high resistance to most hydrolytes, chemicals, and solvents, as such, it is extensively used in the packaging of several kinds of products (Subramanian, 2000).
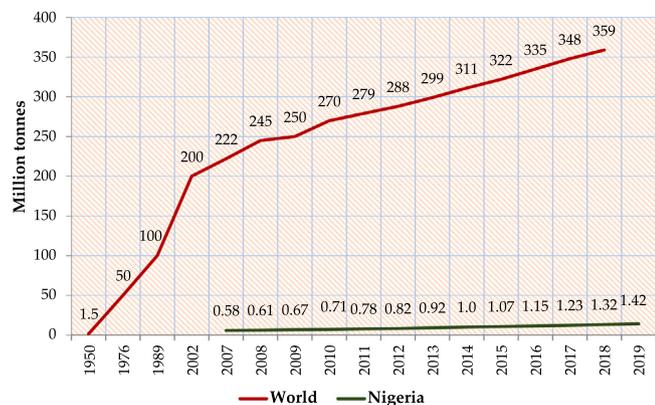
Fig. 1. Annual generation of waste plastics. (Source: (Statista, 2020).

Table 1
Properties of cement used.

Chemical Properties (%) (Source:Bamigboye et al., 2021)	
Al_2O_3	4.44
MgO	2.32
SiO_2	20.71
CaO	62.80
SO_3	2.37
Fe_2O_3	2.78
Cl^-	0.007
$Na_2O + K_2O$	0.88
f-CaO	0.79
Loss of ignition	3.38
Physical Properties	
Final setting time (mins)	540
Initial setting time (mins)	30
Specific gravity	3.15
Surface area (m^2/kg)	364
Consistency (%)	30

Concrete remains the next most used material after water, the ever-rising rate of urbanization has over time resulted in excessive exploitation and depletion of natural resources used in concrete production (Bhardwaj and Kumar, 2017). These resources majorly include sand, gravel, and limestone. Aggregates constitutes between 60% and 80% of the volume of concrete, and greatly influences its properties including permeability, strength, workability, and durability (Faraj et al., 2019). Since large volumes of concrete require substantial quantities of coarse and fine aggregates, the utilization of waste materials in concrete can aid in conserving natural resources while offering a more sustainable solution to the waste disposal concerns.

Among the several techniques in recycling management, the reutilization of waste plastics in building construction is considered the most ideal disposal technique. Here, waste plastics can be reused with no quality degradation during its processing, while substituting the use of fast-depleting natural materials (Almeshal et al., 2020). In the past two decades, several studies have incorporated waste plastics in cementitious composites in the form of aggregates, replacing natural aggregates. these studies have investigated the fresh and hardened properties of the modified composites (Al-Hadithi and Ahmed, 2015; Al-Hadithi and Alani, 2018; Hannawi et al., 2010; Islam et al., 2016; Maharaj et al., 2019; Mohammed and Rahim, 2020; Perera et al., 2019; Sojobi et al., 2016; Remadnia et al., 2009; Mesbah and Buyle-Bodin, 1999; Sikalidis et al., 2002). The use of these waste plastics also achieves a critical goal in the construction industry by significantly reducing the density and deadweight of produced concrete, thereby mitigating earthquake risks (Akçaözoğlu et al., 2010). Other benefits include reduced initial construction costs, and reduced manufacturing and handling times (Colangelo et al., 2016). However, only a limited number of studies have assessed the thermal and microstructural characteristic of this alternative, especially with PET pre-treatment.

This study is designed to assess the effects of recycling waste PET as coarse aggregate in concrete production for building applications. The fresh and hardened properties were assessed with varying percentages of heat-pre-treated PET as a substitute for natural coarse aggregates. The effects of heat-pre-treated PET on the microstructure and thermal characteristics of the produced composites were also assessed. Prediction models were developed utilizing the key parameters studied. The outcomes of this study is targeted at offering a more sustainable material for the production of eco-friendly concrete.

2. Materials and methods

Materials used in this study include: Cement, natural fine and coarse aggregate, and shredded PET. The Dangote brand of cement (grade 42.5 N) served as the binding agent. Table 1 shows the properties of the cement used. Chemical properties were obtained from a past study adopting the same brand of cement (Bamigboye et al., 2021), while the physical properties were obtained from laboratory tests. River sand was collected around the Ogun River to serve as the natural fine aggregates. Clean granite were further aquired from the Igbo-Ora quarry in Nigeria to serve as the natural coarse aggregate whereas shredded PET wastes collected from the Waste-to-Wealth Centre in Covenant University was used in percentages as replacement for natural coarse aggregates. The grain size distribution of all aggregates used are illustrated in Fig. 2.

2.1. Material treatment and preparation

The fine and coarse natural aggregates were cleaned of impurities, dried, and sieved. PET plastic treatment was done by first cleaning and removing all labels and adhesives, shredding the PET plastics into flakes by cutting, then melting at a temperature of about 230 °C. The melted PET mix was then allowed to cool, then crushed with the use of a hammer to maximum sizes of three-quarters of an inch before sieving. Table 2 presents the physical properties of the aggregates used after preliminary testing. Fig. 3 further shows the melting process and the final processed plastic aggregates.

2.2. Mixing and batching

In this study, seven sample blends were assessed. A control blend composed of traditional concrete aggregates, and six PET-modified blends composed of crushed PET and granite in varying proprtions (0:100, 10:90, 20:80, 30:70, 40:60, 50:50, and 100:0), as coarse aggregate. Curing was achieved by submersing all concrete samples in a curing pool filled with potable water for at least 28 days. Fig. 4 explains the adopted experimental program. A mix design ratio of 1:2:4 was implemented to obtain a mean target strength of 25 N/mm^2 for concrete grade 25, with the water/cement ratio fixed at 1/2. For every mix, 3 concrete cylinders (Length = 200 mm
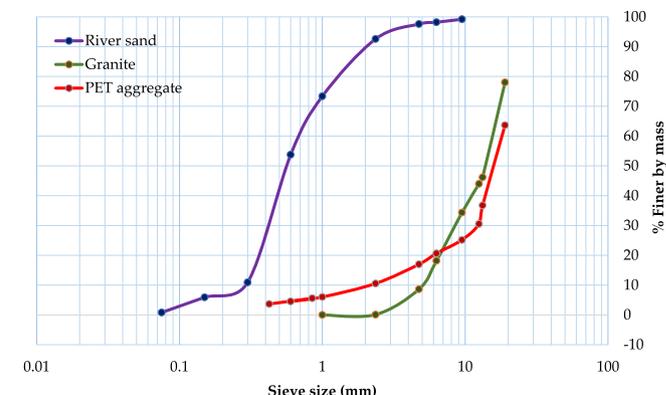
Fig. 2. Aggregates particle size distribution curves.

Table 2
Aggregate properties.

Property	Water absorption (%)	Specific gravity	Crushing value (%)	Impact value (%)	Fineness modulus
River sand	1.2	2.68	–	–	3.67
Recycled waste PET	0.1	–	54.8	53.11	8.76
Granite	0.8	–	27.8	25.11	6

Fig. 3. Crushed plastic after melting.

and Diameter = 100 mm) were used for split tensile strength testing on each test day based on ASTM C496/C496M-17, and 3 concrete cubes (100 mm³) for evaluating the compressive strength according to ASTM C39/C39M-20.

2.3. Tests performed

2.3.1. Workability test

The consistency and ease-of-flow of each freshly mix blend was evaluated via slump cone and compaction factor test methods. These tests were performed following ASTM C143/C143M-15a, 2015a and IS1199–2–2018, respectively. During mixing of individual concrete blends, concrete was placed into a surface-levelled slump cone and then tamped. The cone was then raised and the slump value determined as the height drop between the cone and sample.

2.3.2. Compressive strength tests

Tests for concrete compressive strength were performed after the 3rd, 7th, 14th, and 28th day of water-curing The tests were conducted on the concrete cubes in line with ASTM C39/C39M-20, 2020 with the aid of a compression testing device. Concrete cubes were fitted into the device and the compressive effort was induced at the standard rate until failure was observed. The compressive strength value was then determined for each mix blend based on the corresponding recorded failure loads.

2.3.3. Split tensile strength tests

Concrete split tensile strength tests were conducted on all mix blends after the 3rd, 7th, 14th, and 28th day of water-curing. The tests were conducted on the concrete cylinders in line with ASTM C496/C496M-17, 2017 with the aid of a compression testing device. Concrete samples were horizontally placed in the device with support points along the splitting axis above and beneath. Loading was then induced gradually and constantly at a standard rate until splitting was observed. The split tensile strength value was then determined for each concrete blend based on the corresponding recorded failure loads.

2.3.4. Microstructural analysis

A scanning electron microscope (SEM) LEO 1455VP model was used to investigate the effects of PET addition on the composite's microstructure at 20- and 100%-PET modification levels. SEM generates high-
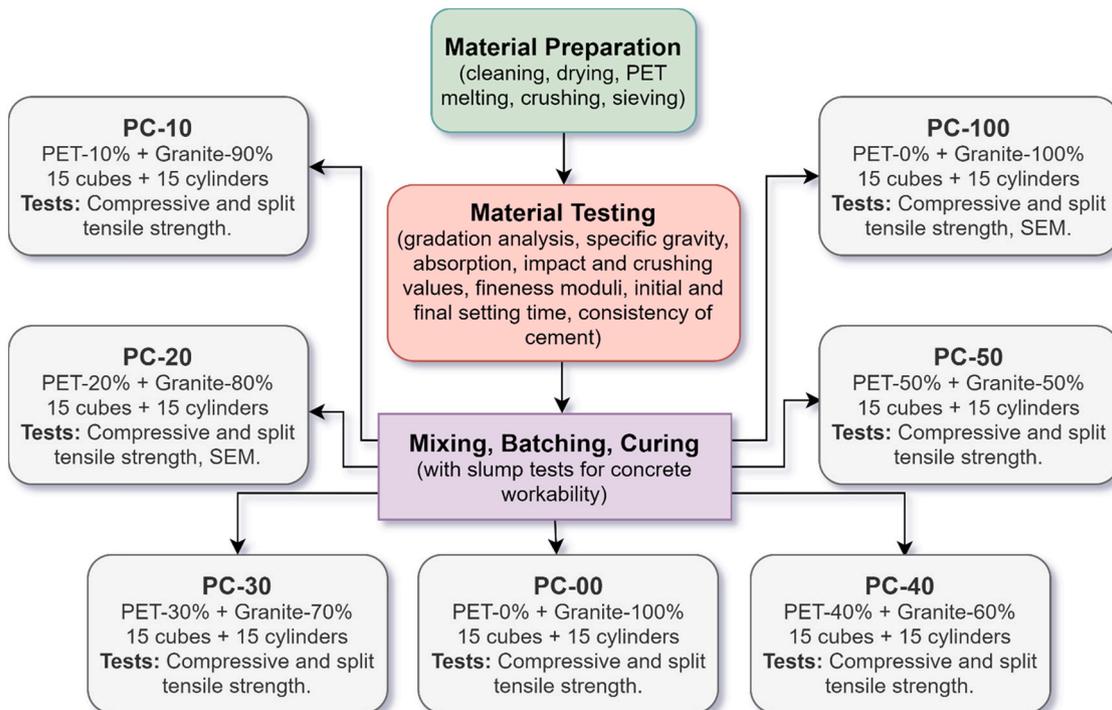
Fig. 4. Experimental program.
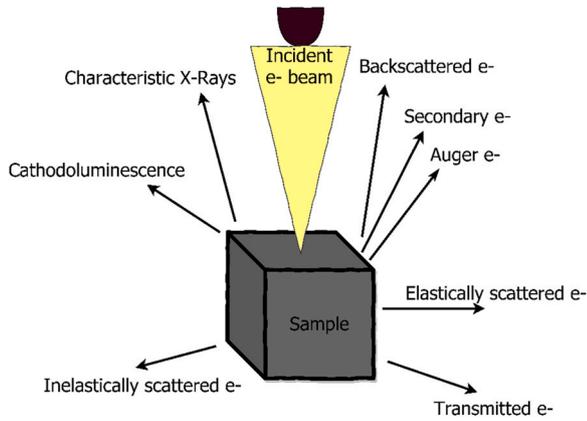
Fig. 5. Illustration of the electron beam-specimen interaction and resultant products.

resolution images of the specimen via the rastering an electron beam concentrated on the specimen's surface and the detection of back-scattered or secondary electron signal. Also, an energy-dispersive X-ray spectroscopy (EDXS) analyser was used for a quantitative identification of the elemental composition of the tested composites. The electron beam-specimen interaction produces a range of signals containing a variety of data on the samples such as cathodoluminescence; indicating the structure of electrons and the chemical composition of the material, secondary electron; for topographic data, and transmitted electron; for a description of the internal structure and crystallography of the material as shown in Fig. 5 (Goldstein et al., 2018).

2.3.5. Thermal analysis

A differential scanning calorimetric (DSC) thermal analysis was performed on the 100% PET modified sample using DSC Q2000 V24.10 model. DSC analysis evaluates the amount of thermal energy absorbed or expelled by a sample during heating or and cooling cycles, it quantitatively and qualitatively produces endothermic (heat absorption) and exothermic (heat evolution) data from thermal processes. The test sample was positioned on a pan and placed on a constantan disc on the DSC analysis cell, a chromel wafer was positioned directly underneath it. The chromel-alumel thermocouple measures the sample temperature. A second control pan, empty, is placed on a symmetric platform directly above a chromel wafer and chromel-alumel thermocouple. The heat flow is computed as the difference in temperature between the test sample and the control chromel wafers according to ASTM E2160-04, 2018.
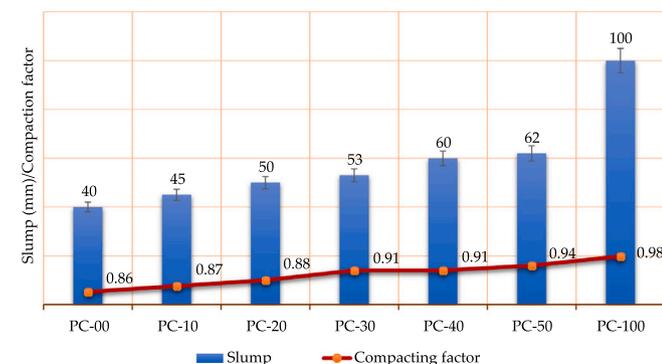
Fig. 6. Slump and compacting factor tests results.

3. Results and discussion

3.1. Workability tests

The Slump cone and compaction factor tests were performed to determine the consistency and workability of the produced concrete. Results presented in Fig. 6 indicate an incessant rise in workability with rising percentages of PET. From the slump test, all PET-based batches indicated allowable workability values for nominal to light reinforcement works (ASTMC143/C143M-15a). All mix blends showed true slumps, except the PC-100 mix, signifying that the addition of PET only results in early-age collapse or shearing of concrete at 100% natural aggregate replacement. The increase in workability can be linked to reduced stiffness as the PET aggregates offer reduced absorption of water, leading to poor bonding between the matrix and the PET. The increasing workability contradicts results seen in past studies recycling PET in different percentages (Coppola et al., 2016; Ferreira et al., 2012; Ismail and AL-Hashmi, 2008; Lee et al., 2019; Rahmani et al., 2013; Silva et al., 2013). However, these studies utilized PET as aggregates without any pre-treatment (melting and crushing) as was the case in this study. The workability results obtained by (Islam et al., 2016), of which a similar PET pre-treatment was adopted, conforms with the increasing trend recorded, even though the PET was heated at 280 °C in that study. The compaction factor test showed a correlation with the slump values as the workability increased from a low degree in the control mix to a high degree in the PC-100 mix.

3.2. Mechanical properties

3.2.1. Compressive strength tests

The evolution of compressive strength after the 3rd, 7th, 14th, 21st, and 28th day of curing across the different mix blends are presented in Fig. 7. The compressive strength steadily developed with the length of curing. However, it gradually reduced as the percentages of PET increased on all test days. On the 14th and 21st days, the least declines observed were up to 56.4% and 56.8% from the PC-10 batch. The 28-day target strength for concrete grade 25 was only reached with the control blend. The PET-modified blends achieved a compressive strength decline of up to 61.7% on the 28th day with the PC-100 mix. Only the PC-20 batch achieved the target strength for concrete grade 20 at 28 days. However, no other PET-modified blend achieved the minimum strength requirements based on ASTM C39/C39M, and are hence not suitable for the production of mass concrete.

The decline in compressive strength can be as a result of the low level of water absorption, and the low impact and crushing resistances, offered by the PET aggregates as indicated in Table 2. Past studies attributed to the decrease in compressive strength with PET additions to the honeycomb formations and the failure modes (Albano et al., 2009). Also, PET additions were seen to decrease the formation of hydration products in the interface thus, decreasing the bonding and compressive strength (Gesoglu et al., 2017). Generally, the decreasing trend observed in this study kow-tows that of past studies employing PET as both coarse and fine aggregates (Gesoglu et al., 2017; Li et al., 2020; Saikia and De Brito, 2014; Silva et al., 2013).

3.2.2. Split tensile strength tests

Split tensile strength tests were conducted after the 3rd, 7th, 14th, 21st, and 28th day of curing. The results obtained are presented in Fig. 8. Split tensile strength increased slightly with curing age, and decreased gradually with the addition of PET at all curing stages. Initial tensile strength values on the 3rd and 7th day for the 10% and 20% PET-modified batches were slightly higher than that of the unmodified batch (PC-00), this observation was similar to results from (Needhidasan et al., 2020). However, the results after the 14th, 21st, and 28th day indicated an upsurge in strength for the PC-00 batch and a decline with PET percentages, only the PC-10 and PC-20 batches achieved substantial tensile strength values. Of all the PET-modified
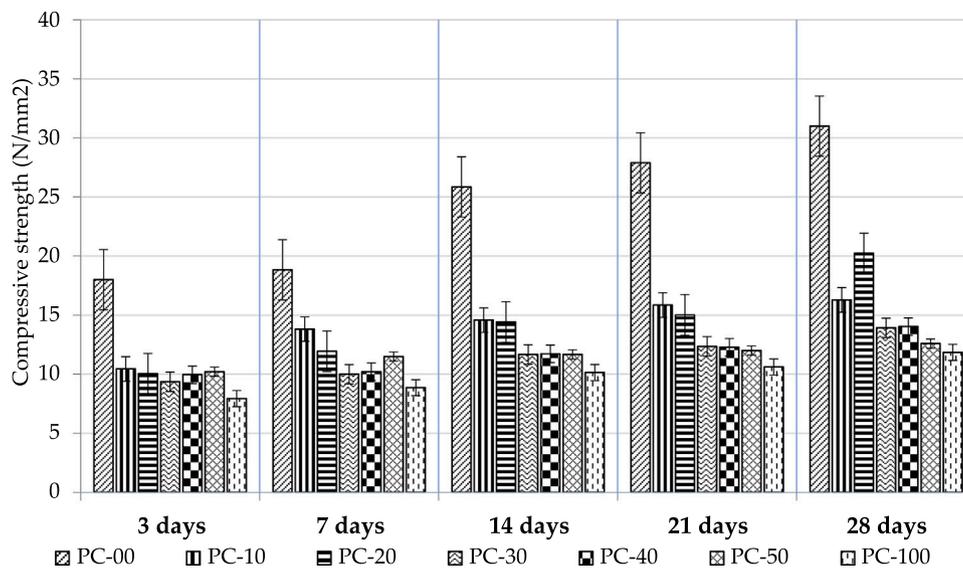
Fig. 7. Compressive strength tests results.
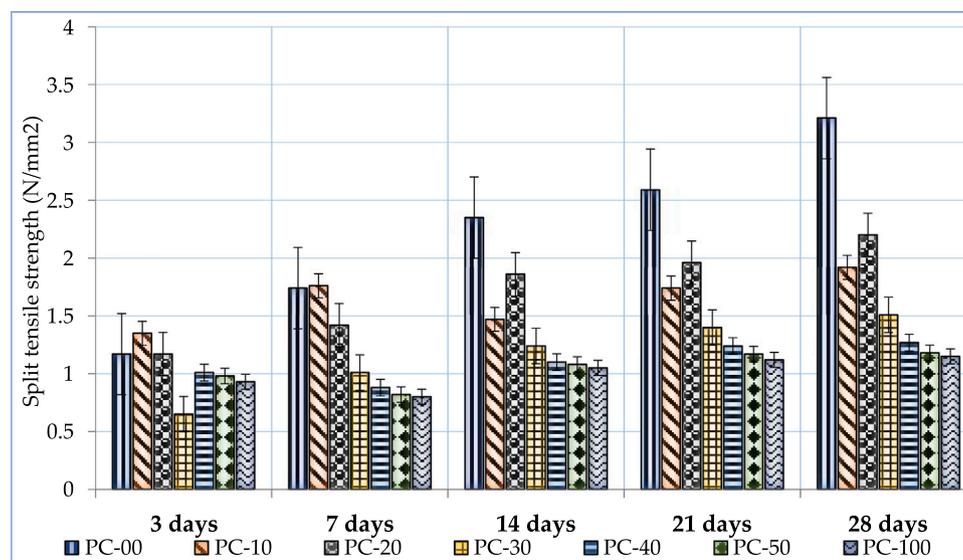
Fig. 8. Split tensile strength tests results.

batches, the PC-20 batch achieved the highest tensile strength (2.2 N/mm^2) after the 28th day, and based on ASTM C496/C496M-17, it falls within the recommended limits for mass concrete production.

The split tensile strength is more influenced by bonding quality and less by particle size (Ferreira et al., 2012; Saikia and De Brito, 2014). The tensile strength decrease was also attributed to the smoother surface texture and greater surface area of the PET aggregate, resulting in weaker bonding at the interface and free water accumulation (Li et al., 2020; Sharma and Bansal, 2016). The 10% and 20% PET-modified mixes showed higher plasticity and flexibility due to the flexible nature of plastic, resulting in a less-brittle failure (Sadrmomtazi et al., 2016). However, the decline in tensile strength was apparently due to the weaker bonds between the matrix and the PET aggregates.

3.3. Microstructural analyses results

3.3.1. Scanning electron microscopy (SEM)

To acquire further information on the effect of PET on the surface structure of the produced composite, SEM experimentations were performed on the PC-100 and PC-20 samples. The resulting microstructural graphs are presented in Fig. 9. The morphology of the PC-100 sample indicated a relatively irregular form. Pores of about 2–4 µm were noticed on the exterior of PC-100, multiple bright inclusions (cement formations) encircled by hydrating agents such as C-S-H were observed on the surface improving the bonding between the PET aggregates and the matrix. Micro extrusions of the PET aggregates were also noticed indicating slight honeycombing in the PC-100 sample. However, the presence of microcracks were not observed.

The SEM on the PC-20 indicated a much denser interface between the PET aggregates and the cement matrix. The pores are seen clearly in Fig. 9B because of the deeper degree of magnification as noticed in the Selected Area 3. There were cement formations on a wider area compared to the PC-100 sample. No microcracks were observed in the sample.

3.3.2. Energy-dispersive X-ray spectroscopy (EDXS)

A fundamental understanding of the effect of PET on the surface structure of the produced composites has been carried out using the

(A) PC-100   **(B)** PC-20
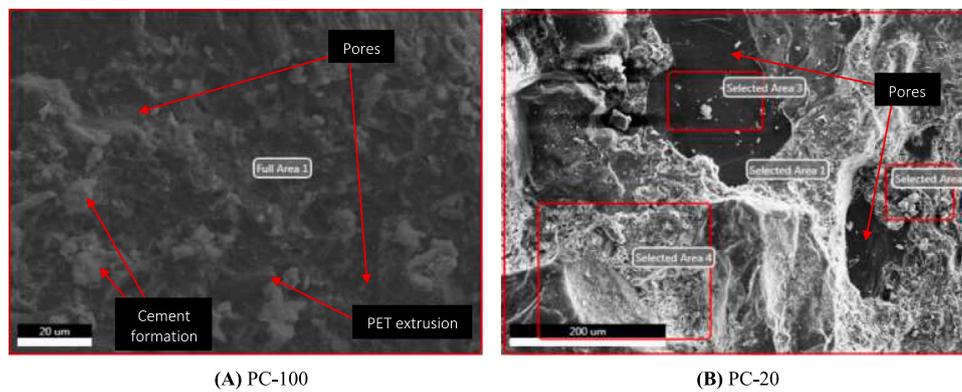
Fig. 9. SEM micrographs of samples after 28 days.
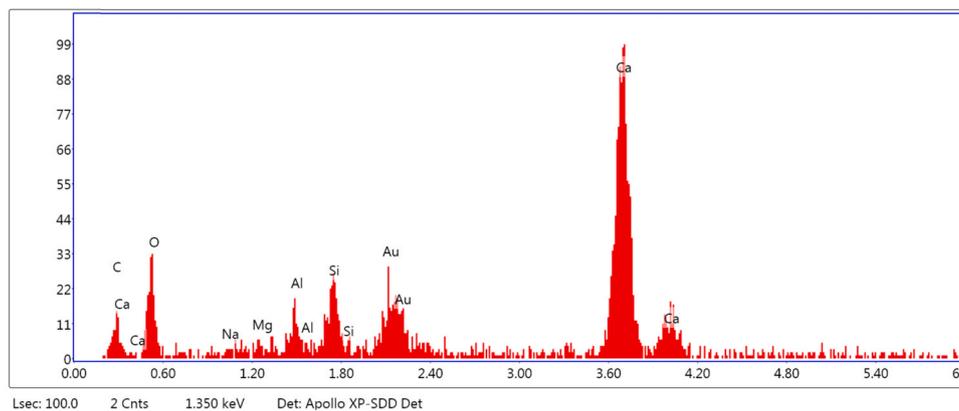
Fig. 10. EDXS spectrum of PC-100 after 28 days.

SEM analysis. However, to qualitatively and quantitatively determine the elemental composition of the composites, EDXS was conducted at the selected areas of interest on the PC-20 and PC-100 samples shown indicated in Fig. 9. The EDXS revealed that the chemical composition of individual samples differs at multiple spots as a result of the different emissions from the characteristic X-rays. The EDXS results and spectrum peaks are presented in Fig. 10 and Fig. 11. EDXS on the PC-100 shows a great percentage of Ca and minor quantities of O, C, Au, Al, Si, Mg, and Na. On the other hand, the PC-20 indicated high quantities of Si, O, and Ca, and moderate to minor quantities of Al, Au, Na, and Mg, at all selected areas. The higher percentage of Si and O in the PC-20 is due to the lower quantity of PET in the sample.

3.4. Thermal analysis results

Thermal analysis was conducted using a differential scanning calorimetry (DSC) to evaluate the temperature and heat flow through the PC-100 sample. The DSC result is indicated in Fig. 12, and provides quantitative and qualitative data on the exothermic/endothermic processes or heat capacity changes. At an average of 10 °C/min heating rate, the process began at 25 °C. During the process, a glass transition was noticed with an onset temperature of 62.5 °C and a midpoint T_g of 73.2 °C. An exothermic peak below decomposition temperature during heating was noticed at a temperature 194.76 °C, this can be as a result of the curing or crystallization of the PET in the sample. Also, a baseline shift was observed after the endothermic peak at 242.71 °C, this can be attributed to reasons like changes in either the heating rate, sample weight, or the sample's specific heat. Specific heat change of the sample can occur after the sample undergoes crystallization, curing, or melting (Shawe et al., 2000; TA Instruments, 2010).

4. Statistical analysis

4.1. Correlation and regression between workability and mechanical properties

Bivariate Pearson correlation tests were performed to determine whether any kind of variation exists across the parameters assessed. The coefficients of correlation are presented in Table 3. PET% showed significant negative correlations with split tensile strength (R = −0.716) and compressive strength (R = −0.668), and a very high positive correlation with the slump (R = 0.989) and compaction factor (R = 0.978). Compressive strength likewise indicated a high positive correlation with split tensile strength (R = 0.952), and significant negative correlations with slump (R = −0617) and compaction factor (R = −0.738). The split tensile strength values gave significant negative correlations with both workability parameters.

A series of bivariate regressional analysis were performed to measure the interdependence between the strength and workability parameters assessed. A box plot was used for the inspection, and no outliers were found in the measured values. The values of each dependent variable were assessed using a Shapiro-Wilk test of normality (p > 0.05), a normal distribution was observed for all three variable datasets. There was no violation of homogeneity of variance based on Levene's equality test. From the one-way ANOVA ($F(6,14) = 34.718$, $p < 0.0011$), there was a statistically significant difference between the means. A Turkey post hoc test showed that the compressive strength was statistically significantly lower after taking the PC-100 (10.86 ± .879 min, $p < 0.001$) and PC-30 (12.67 ± 1.15 min, $p < 0.001$) batches compared to the PC-00 batch (28.24 ± 2.58 min). there was no statistically significant difference between the PC-10 and PC-20 batches ($p = 0.992$).
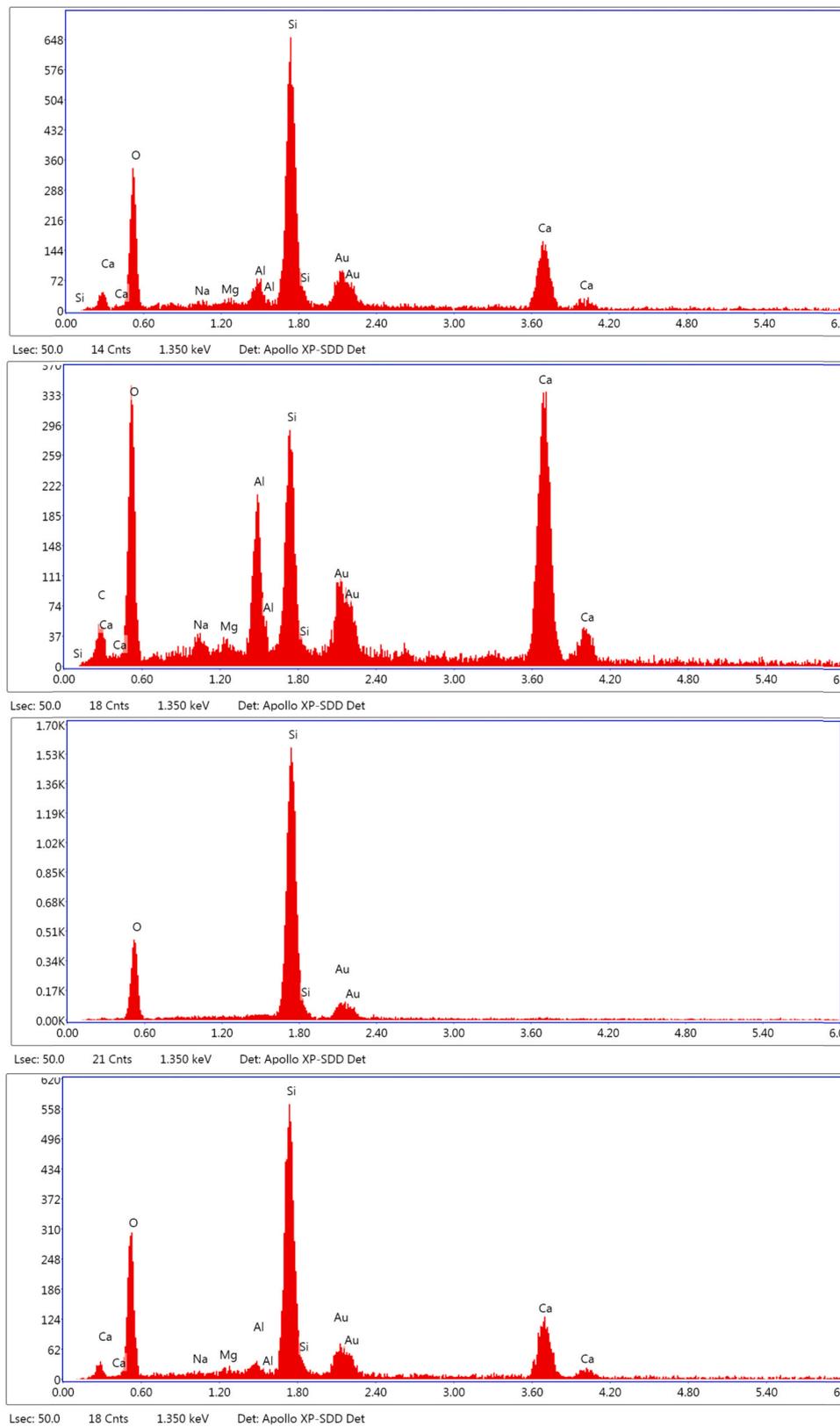
Fig. 11. EDXS spectrum for PC-20 after 28 days at selected areas (A) 1 (B) 2 (C) 3 (D).
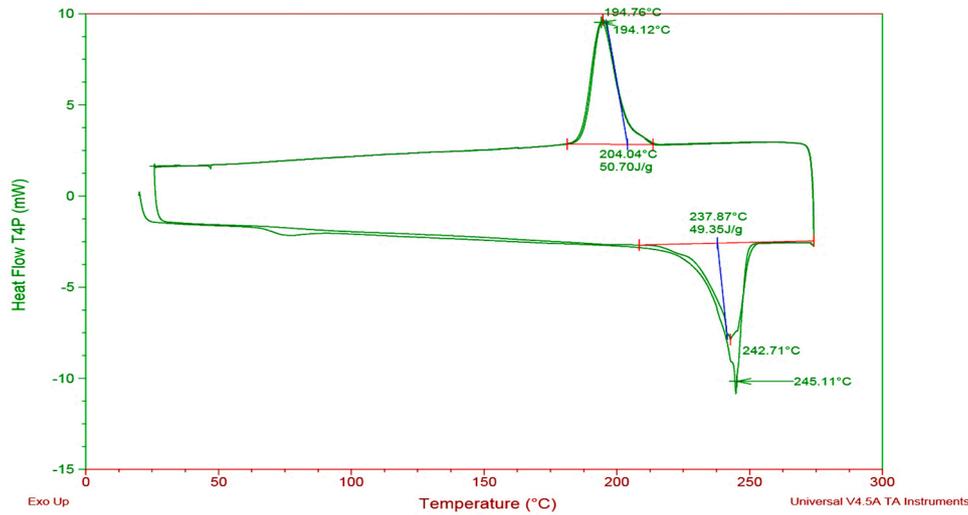
Fig. 12. DSC scan on PC-100 after quench cooling.

Table 3
Correlation coefficients (R).

Variables	Compressive strength	Split tensile strength	Slump value	Compaction factor
PET %	-0.668**	-0.716**	0.989**	0.978**
Compressive strength	1	0.952**	-0.617	-0.738
Split tensile strength	–	1	-0.670	-0.803*
Slump value	–	–	1	0.939**
Compaction factor	–	–	–	1

* *. Correlation is significant at the 0.01 level (2-tailed).
* . Correlation is significant at the 0.05 level (2-tailed)
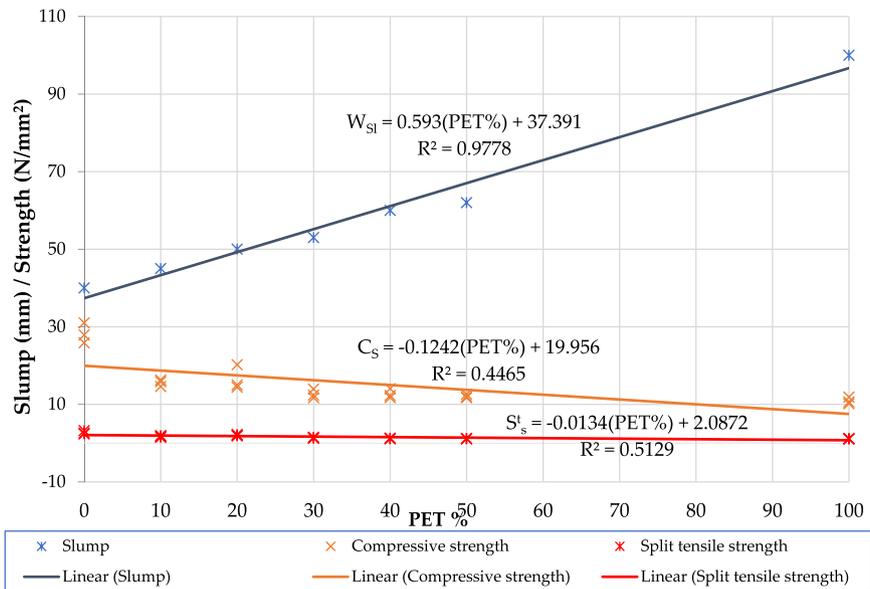
Fig. 13. Relationships between workability, compressive strength, split tensile strength and PET %.

The trend and variations from the regression of Compressive strength (C_S), split tensile strength (S_S^t), and workability (W_{Sl}) on PET% are presented in Fig. 13, while that from the regression of S_S^t on C_S is shown in Fig. 14. Linear functions established with PET% as predictor for C_S and S_S^t indicated low-significance coefficients of dependence (R^2) of 0.4465 and 0.5129, respectively. While a linear function with R^2 = 0.997 was established for W_{Sl} with PET% as the predictor. This showed that the split tensile strength, and workability values obtained are adequately described by the PET percentage data. The low R^2-value indicated for the C_S and data is resultant of the low-significance R value shown in Table 3. The regression of S_S^t with C_S as a predictor also showed lineraity with R^2 = 0.8402, indicating high significance as shown in Fig. 14. The variations established are detailed in Table 4.
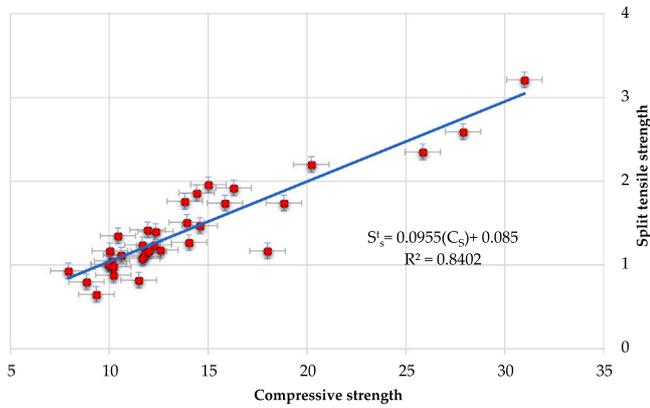
Fig. 14. Relationship between split tensile strength and compressive strength.

4.2. Validation of models

The prediction models developed were validated further. The model validation results are presented in Table 5. The compressive and split tensile strength prediction models using PET% as the predictor indicated the highest error margins, this is explained by the low R^2 values obtained from the linear regression. The workability (slump) prediction model with PET% as the predictor, and the split tensile strength prediction model with compressive strength as predictor both indicated very low error margins of 0.223% and 0.875%, respectively.

4.3. Economic model appraisal

The economic analysis of the mechanical, microstructural and thermal characteristics of concrete with waste PET as coarse aggregates was examined with its associated costs as shown in Table 6. The model explanatory strength at 76.3% and 84.6% indicate a high fitness level while the global significance of the model (F-statistics $= 9.565$, p-value < 0.05; $16.443 < 0.05$) was confirmed at 5% significance level.

Evidence from the comprehensive strength reveals that only 14-days and 21 days comprehensive strength were significantly related with the proportions of PET and granite mix utilized.

The analysis of the 14-days comprehensive strength test shows on the average that a unit rise in PET cost has a decreasing effect of $0.874\,\text{N/mm}^2$ on comprehensive strength of concrete while the cost of granite was found to be positively related with concrete strength at same rate $0.874\,\text{N/mm}^2$ increasing effect. The statistical test of significance and model reliability (ANOVA) result confirmed this at 5% significance level.

The 21-days result further confirmed this result with PET retarded effect of $0.920\,\text{N/mm}^2$ in contrast with granite result of the same magnitude but positive effect at 5% significance level.

The total variation in split tensile strength explained by the cost of PET for the 14-days and 21-days were 67.9% and 69.3% while 98.8%

and 93.5% variations in slump and compaction test were attributed to the changes in PET and granite mix. The F-statistics results (9.665, p-value < 0.05; 16.443, p-value < 0.05; $9.459 < 0.05$; $10.031 < 0.05$; $246.857 < 0.01$ and $42.857 < 0.01$) support the model statistical relevancy and reliability of the estimates.

The workability test indicates a reverse outcome such that a unit increase in the cost of PET increases slump by 0.994 but significantly retards split tensile strength by 0.871 while cost of granite (GRNTC) was negatively influenced slump at the same magnitude of $0.994\,\text{N/mm}^2$ and enhances split tensile strength. Hence, the utilization of PET increases slump result while the cost of granite retards slump by the same measure. In the same vein a naira input as a result of increase in proportion of PET increases compaction factor by $0.967\,\text{N/mm}^2$ while higher granite expenditure revealed no supportive impact on compaction factor. It is therefore more economical to use PET for a more

Table 5
Model validation exercise results.

Predictor value	Measured value(y_m)	Predicted Value (y_p)	Error ($y_m - y_p$)	Mean error (%)
Compressive strength / PET% prediction model ($C_S = -0.1242(PET\%) + 19.956$)				
0	30.99	19.956	11.034	4.859
10	16.29	18.714	-2.424	
20	20.22	17.472	2.748	
30	13.92	16.230	-2.31	
40	14.03	14.988	-0.958	
50	12.59	13.746	-1.156	
100	11.84	7.536	4.304	
Slump / PET% prediction model for workability ($W_{Sl} = 0.593(PET\%) + 37.391$)				
0	40	37.391	2.609	0.223
10	45	43.321	1.679	
20	50	49.251	0.749	
30	53	55.181	-2.181	
40	60	61.111	-1.111	
50	62	67.041	-5.041	
100	100	96.691	3.309	
Split tensile strength / PET% prediction model ($S_S^t = -0.0134(PET\%) + 2.0872$)				
0	3.21	2.087	1.123	5.403
10	1.92	1.953	-0.033	
20	2.2	1.819	0.381	
30	1.51	1.685	-0.175	
40	1.27	1.551	-0.281	
50	1.18	1.417	-0.237	
100	1.15	0.747	0.403	
Split tensile strength / compressive strength prediction model ($S_S^t = 0.0955(C_S) + 0.085$)				
30.99	3.21	3.045	0.165	0.875
16.29	1.92	1.641	0.279	
20.22	2.2	2.016	0.184	
13.92	1.51	1.414	0.096	
14.03	1.27	1.425	-0.155	
12.59	1.18	1.287	-0.107	
11.84	1.15	1.216	-0.066	

Table 4
Summary of regression analysis.

Variables		Prediction Model	Statistical Coefficients	
Criterion	Predictor		R	R^2
W_{Sl}	PET%	$W_{Sl} = 0.593(PET\%) + 37.391$	0.989	0.9788
C_S	PET%	$C_S = 0.0031(PET\%)^2 - 0.4445(PET\%) + 24.453$	-0.668	0.4465
S_S^t	PET%	$S_S^t = -0.000003(PET\%)^3 + 0.0008(PET\%)^2 - 0.0601(PET\%) + 2.5962$	-0.716	0.5129
S_S^t	C_S	$S_S^t = 0.0955(C_S) + 0.085$	0.952	0.8402

Table 6

Model cost analysis.

Cost Analysis	Comprehensive Strength Analysis		Split tensile strength		Workability Test Analysis	
Predictors Mix Proportion: PET /Granite costs	14-Days	21 Days	14-Days	21 Days	Slump	Compaction Factor
Constant	15.368 * **	16.628 * **	2.060 * **	2.339 * **	83.210 * **	0.832 * **
Coefficients	-0.874 * *	-0.920 * *	-0.871 * *	-0.877 * *	0.994 * **	0.967 * **
R-squared	0.763	0.846	0.759	0.770	0.988	0.935
Adjusted R	0.684	0.794	0.679	0.693	0.984	0.913
F-Statistics	9.665 * *	16.443 * *	9.459 * *	10.031 * *	246.857 * **	42.857 * **

Note: * ** , * * represents significance at 1% and 10% level

effective slump outcome and granite for better comprehensive strength and compaction factor result.

5. Environmental and economic impacts

From an environmentalist standpoint, based on the statistic that waste PET constitutes 50–60% of all waste plastics (Rahman and Wahab, 2013) and the outcomes from this study, single-used PET bottle wastes can be considered for modifying concrete. The utilization of these wastes in building construction and rehabilitation operations would meaningfully remove several million tons of PET wastes from landfills and other waste streams. Thereby posing positive impacts on the environment like reduced eyesores and environmental pollutions, reduced CO_2 emissions, controlled drainage issues with PET blockages, prolonged serviceability of landfills, and conservation of natural aggregates used in concrete production. It also promotes a balance in the ecosystem by preventing the bio-accumulation of polymers in the food chain, and with the extraction of the non-biodegradable and inorganic waste PET from the ecosystem (Sojobi et al., 2016). Similarly, the utilization of PET in concrete production can significantly reduce the costs of building construction and maintenance with the reduced material cost, while providing revenues for waste managers. Therefore, there's a need for policies and regulations to enact and monitor the utilization of these wastes in both developed and developing countries as is already in practice in the UK (Kakar et al., 2015).

6. Conclusions

This research portrays the importance of eco-friendly building construction in the pursuit of sustainability in the 21st century. Likewise, this paper assessed the implications of recycling waste PET plastics as a full or partial replacor for natural coarse aggregates, on the fresh and hardened properties, alongside the microstructural and thermal properties of concrete. A mix design ratio of 1:2:4 was implemented to obtain a mean target strength of 25 N/mm² for concrete grade 25, with the water/cement ratio fixed at 1/2. Based on the Laboratory results obtained, the following deductions were made:

i. With increasing content of waste PET, the consistency and workability of the concrete increases. However, all PET blends achieved workability results suitable for low to nominal reinforcement works.
ii. The compressive strength steadily developed with the length of curing. However, it gradually reduced as the percentages of PET increased on all test days. The 28-day target strength for concrete grade 25 was only reached with the control blend. Only the PC-20 batch achieved the target strength for concrete grade 20 at 28 days.
iii. With curing age, split tensile strength increased slightly but decreased steadily with the addition of PET at all curing stages. Initial tensile strength values on the 3rd and 7th days for the 10% and

20% PET-modified batches were slightly higher than that of the unmodified batch (PC-00), Of all the PET-modified batches, the PC-20 batch achieved the highest tensile strength (2.2 N/mm²) after 28 days
iv. Workability showed a high positive correlation with PET percentage. Whereas split tensile strength and compressive strength showed low-significance positive correlations with PET percentage. Regression analysis indicated high-significance linear dependencies between both workability and PET-% (R^2 = 0.9788), and split tensile strength and compressive strength (R^2 = 0.8402) with PET modification.
v. SEM micrographs revealed that the PC-100 sample has a relatively irregular form with pores of about 2–4 μm on its surface. Cement formations encircled by C-S-H improves the bonding between the PET aggregates and the matrix. Micro extrusions of the PET indicate slight honeycombing in the PC-100 sample. The PC-20 had a much denser interface between the PET aggregates and the cement matrix.
vi. EDXS on the PC-100 shows a great percentage of Ca and minor quantities of O, C, Au, Al, Si, Mg, and Na. On the other hand, the PC-20 had high quantities of Si, O, and Ca, and moderate to minor quantities of Al, Au, Na, and Mg. The higher percentage of Si and O in the PC-20 is due to the lower quantity of PET in the sample. Hence, Si and O quantities reduces with increasing PET percentage.
vii. The DSC thermal graph indicates that the sample endured three transition stages. A glass transition with an onset temperature of 62.5 °C and a midpoint T_g of 73.2 °C, an exothermic peak below decomposition temperature during cooling was noticed at a temperature of 194.76 °C from the crystallization of the PET in the sample, and a baseline shift after the endothermic peak at 242.71 °C during the heating run.

Declaration of Competing Interest

The authors declare that they have no known competing financial interests or personal relationships that could have appeared to influence the work reported in this paper.

References

Akçaözoğlu, S., Atiş, C.D., Akçaözoğlu, K., 2010. An investigation on the use of shredded waste PET bottles as aggregate in lightweight concrete. Waste Manag. 30 (2), 285–290. https://doi.org/10.1016/j.wasman.2009.09.033

Al-Hadithi, A.I., Ahmed, M., 2015. Mechanical properties of high performance concrete containing waste plastic as aggregate. Univ. Baghdad Eng. J. 21, 100–115. ⟨https://www.researchgate.net/publication/285590702_Mechanical_Properties_of_High_Performance_Concrete_Containing_Waste_Plastic_as_Aggregate⟩.

Al-Hadithi, A.I., Alani, M.F., 2018. Importance of adding waste plastics to high-performance concrete. Waste Resource Manag. 171 (2), 36–51. https://doi.org/10.1680/JWARM.17.00040

Albano, C., Camacho, N., Hernández, M., Matheus, A., Gutiérrez, A., 2009. Influence of content and particle size of waste pet bottles on concrete behavior at different w/c ratios. Waste Manag. 29 (10), 2707–2716. https://doi.org/10.1016/j.wasman.2009.05.007

Almeshal, I., Tayeh, B.A., Alyousef, R., Alabduljabbar, H., Mustafa Mohamed, A., Alaskar, A., 2020. Use of recycled plastic as fine aggregate in cementitious composites: a review. Construct. Build. Mater. https://doi.org/10.1016/j.conbuildmat.2020.119146

ASTM C39/C39M-20, 2020. Standard Test Method for Compressive Strength of Cylindrical Concrete Specimens. ASTM International, West Conshohocken, PA

ASTM C143/C143M-15a, 2015a. Standard Test Method for Slump of Hydraulic-Cement Concrete.

ASTM C496/C496M-17, 2017. Standard Test Method for Splitting Tensile Strength of Cylindrical Concrete Specimens. ASTM International, West Conshohocken, PA. https://doi.org/10.1520/C0496_C0496M-17.

ASTM E2160-04, 2018. Standard Test Method for Heat of Reaction of Thermally Reactive Materials by Differential Scanning Calorimetry. ASTM International, West Conshohocken, PA. https://doi.org/10.1520/E2160-04R18.

Bamigboye, G.O., Ngene, B.U., Ademola, D., Jolayemi K., J., 2019. Experimental study on the use of waste Polyethylene Terephthalate (PET) and River sand in roof tile production. Journal of Physics: Conference Series 1378. https://doi.org/10.1088/1742-6596/1378/4/042105

Bamigboye, G.O., Tarverdi, K., Wali, E.S., Bassey, D.E., Jolayemi, K.J., 2021. Effects of dissimilar curing systems on the strength and durability of recycled PET-modified concrete. Silicon 2021, 1–13. https://doi.org/10.1007/S12633-020-00898-0

Bhardwaj, B., Kumar, P., 2017. Waste foundry sand in concrete: a review. Constr. Build. Mater. 661–674. https://doi.org/10.1016/j.conbuildmat.2017.09.010

Colangelo, F., Cioffi, R., Liguori, B., Iucolano, F., 2016. Recycled polyolefins waste as aggregates for lightweight concrete. Compos. B Eng. 106, 234–241. https://doi.org/10.1016/j.compositesb.2016.09.041

Coppola, B., Courard, L., Michel, F., Incarnato, L., Di Maio, L., 2016. Investigation on the use of foamed plastic waste as natural aggregates replacement in lightweight mortar. Compos. B Eng. 99, 75–83. https://doi.org/10.1016/j.compositesb.2016.05.058

Faraj, R.H., Sherwani, A.F.H., Daraei, A., 2019. Mechanical, fracture and durability properties of self-compacting high strength concrete containing recycled polypropylene plastic particles. J. Build. Eng. 25, 100808. https://doi.org/10.1016/j.jobe.2019.100808

Ferreira, L., De Brito, J., Saikia, N., 2012. Influence of curing conditions on the mechanical performance of concrete containing recycled plastic aggregate. Constr. Build. Mater. 36, 196–204. https://doi.org/10.1016/j.conbuildmat.2012.02.098

Gesoglu, M., Güneyisi, E., Hansu, O., Etli, S., Alhassan, M., 2017. Mechanical and fracture characteristics of self-compacting concretes containing different percentage of plastic waste powder. Constr. Build. Mater. 140, 562–569. https://doi.org/10.1016/j.conbuildmat.2017.02.139

Goldstein, J.I., Newbury, D.E., Michael, J.R., Ritchie, N.W.M., Scott, J.H.J., Joy, D.C., 2018. Scanning Electron Microscopy and X-Ray Microanalysis, fourth ed. Springerhttps://doi.org/10.1007/978-1-4939-6676-9

Hannawi, K., Prince, W., Kamali-Bernard, S., 2010. Effect of thermoplastic aggregates incorporation on physical, mechanical and transfer behaviour of cementitious materials. Waste Biomass Valoriz. 2 (1), 251–259. https://doi.org/10.1007/S12649-010-9021-Y

Islam, M.J., Meherier, M.S., Islam, A.K.M.R., 2016. Effects of waste PET as coarse aggregate on the fresh and harden properties of concrete. Constr. Build. Mater. 125, 946–951. https://doi.org/10.1016/j.conbuildmat.2016.08.128

Ismail, Z.Z., AL-Hashmi, E.A., 2008. Use of waste plastic in concrete mixture as aggregate replacement. Waste Manag. 28 (11), 2041–2047. https://doi.org/10.1016/j.wasman.2007.08.023

Kakar, M.R., Hamzah, M.O., Valentin, J., 2015. A review on moisture damages of hot and warm mix asphalt and related investigations. J.Clean. Prod. https://doi.org/10.1016/j.jclepro.2015.03.028

Lee, Z.H., Paul, S.C., Kong, S.Y., Susilawati, S., Yang, X., 2019. Modification of waste aggregate PET for improving the concrete properties. Adv. Civil Eng. https://doi.org/10.1155/2019/6942052

Li, X., Ling, T.C., Hung Mo, K., 2020. Functions and impacts of plastic/rubber wastes as eco-friendly aggregate in concrete – a review. Constr. Build. Mater. https://doi.org/10.1016/j.conbuildmat.2019.117869

Maharaj, R., Maharaj, C., Mahase, M., 2019. The performance and durability of polyethylene terephthalate and crumb rubber-modified road pavement surfaces. Prog. Rubber Plast. Recycl. Technol. 35 (1), 3–22. https://doi.org/10.1177/1477760618798425

Mesbah, H., Buyle-Bodin, F., 1999. Efficiency of polypropylene and metallic fibres on control of shrinkage and cracking of recycled aggregate mortars. Constr. Build. Mater. 13 (8), 439–447.

Mohammed, A.A., Rahim, A.A.F., 2020. Experimental behavior and analysis of high strength concrete beams reinforced with PET waste fiber. Constr. Build. Mater. 244, 118350. https://doi.org/10.1016/j.conbuildmat.2020.118350

Needhidasan, S., Ramesh, B., Joshua Richard Prabu, S., 2020. Experimental study on use of E-waste plastics as coarse aggregate in concrete with manufactured sand. Mater. Today. Proc. 22, 715–721. https://doi.org/10.1016/j.matpr.2019.10.006

Panyakapo, P., Panyakapo, M., 2008. Reuse of thermosetting plastic waste for lightweight concrete. Waste Manag. 28 (9), 1581–1588. https://doi.org/10.1016/j.wasman.2007.08.006

Perera, S., Arulrajah, A., Wong, Y.C., Horpibulsuk, S., Maghool, F., 2019. Utilizing recycled PET blends with demolition wastes as construction materials. Constr. Build. Mater. 221, 200–209. https://doi.org/10.1016/j.conbuildmat.2019.06.047

Rahmani, E., Dehestani, M., Beygi, M.H.A., Allahyari, H., Nikbin, I.M., 2013. On the mechanical properties of concrete containing waste PET particles. Constr. Build. Mater. 47, 1302–1308. https://doi.org/10.1016/j.conbuildmat.2013.06.041

Rahman, W.M.N.W.A., Wahab, A.F.A., 2013. Green pavement using recycled Polyethylene Terephthalate (PET) as partial fine aggregate replacement in modified asphalt. Procedia Eng. 53, 124–128. https://doi.org/10.1016/j.proeng.2013.02.018

Remadnia, A., Dheilly, R.M., Laidoudi, B., Quéneudec, M., 2009. Use of animal proteins as foaming agent in cementitious concrete composites manufactured with recycled PET aggregates. Constr. Build. Mater. 23 (10), 3118–3123.

Sadrmomtazi, A., Dolati-Milehsara, S., Lotfi-Omran, O., Sadeghi-Nik, A., 2016. The combined effects of waste Polyethylene Terephthalate (PET) particles and pozzolanic materials on the properties of selfcompacting concrete. J.Clean. Prod. 112, 2363–2373. https://doi.org/10.1016/j.jclepro.2015.09.107

Saikia, N., De Brito, J., 2014. Mechanical properties and abrasion behaviour of concrete containing shredded PET bottle waste as a partial substitution of natural aggregate. Constr. Build. Mater. 52, 236–244. https://doi.org/10.1016/j.conbuildmat.2013.11.049

Sharma, R., Bansal, P.P., 2016. Use of different forms of waste plastic in concrete - a review. J. Clean. Prod. 112, 473–482. https://doi.org/10.1016/j.jclepro.2015.08.042. (Elsevier Ltd).

Shawe, J., Riesen, R., Widmann, J., Schubnell, M. , 2000 , Interpreting DSC curves Part 1: Dynamic measurements. In *Information for users of METTLER TOLEDO thermal analysis systems*.

Siddique, R., Khatib, J., Kaur, I., 2008. Use of recycled plastic in concrete: a review. Waste Manag. 28 (10), 1835–1852. https://doi.org/10.1016/j.wasman.2007.09.011

Sikalidis, C.A., Zabaniotou, A.A., Famellos, S.P., 2002. Utilisation of municipal solid wastes for mortar production. Res. Conserv. Recycl. 36 (2), 155–167.

Silva, R.V., De Brito, J., Saikia, N., 2013. Influence of curing conditions on the durability-related performance of concrete made with selected plastic waste aggregates. Cement Concr. Compos. 35 (1), 23–31. https://doi.org/10.1016/j.cemconcomp.2012.08.017

Sojobi, A.O., Nwobodo, S.E., Aladegboye, O.J., 2016. Recycling of polyethylene terephthalate (PET) plastic bottle wastes in bituminous asphaltic concrete. Cogent Eng. 3 (1), 1–28. https://doi.org/10.1080/23311916.2015.1133480

Statista , 2020 , Global plastic production | Statista. ⟨https://www.statista.com/statistics/282732/global-production-of-plastics-since-1950/⟩.

Subramanian, P.M., 2000. Plastics recycling and waste management in the US. Res. Conserv. Recycl. 28 (3–4), 253–263. https://doi.org/10.1016/S0921-3449(99)00049-X

TA Instruments, 2010 , Interpreting Unexpected Events and Transitions in DSC Results. In TA039.

US Environmental Protection Agency (EPA), 2017 , Advancing Sustainable Materials Management: 2017 Fact Sheet (Issue November). ⟨https://doi.org/10.1017/CBO9781107415324.004⟩.